Pergamon

0042-6989(94)00296-7

Vision Res. Vol. 35, No. 15, pp. 2157–2167, 1995

0042-6989/95 $9.50 + 0.00

Phase-reversal Discrimination in One and Two Dimensions: Performance is Limited by Spatial Repetition, not Spatial Frequency Content

T. S. MEESE*†

Received 20 June 1994; in revised form 11 November 1994

Lawden [(1983) *Vision Research, 23*, 1451–1463] used vertical gratings containing two frequencies (*F*, *nF*) in phase discrimination ($F + nF$ against $F - nF$) and compound detection ($F + nF$ against F) experiments, where thresholds were measured by manipulating the contrast of the *nF* component. When *n* was varied, Lawden found a *phase-plateau* of moderate breadth where phase discrimination thresholds were about half of those measured in compound detection. I present the results of similar experiments, using one-dimensional (gratings) and two-dimensional (plaids). In a sine-plaid condition, the 1*F* grating was split into two 1*F* plaid components at ±45 deg from vertical while the *nF* component remained a vertical grating. In a square-wave plaid (SqW-plaid) condition the plaid components were square waves. For each of these conditions, the horizontal spatial repetition (SR) of the plaid is given by ($F/\sqrt{2}$); it is half an octave lower than the spatial frequency (SF) of the oblique components but it is not represented in the stimulus spectrum. By plotting phase discrimination relative to compound detection a phase-plateau was found for all three conditions. When these data were plotted as a function of SF ratio (*nF*/*F*) the curves describing the two plaid conditions were found to be leftward translations of that describing the grating condition. However, when the results were plotted as a function of SR ratio (*nF*/SR), the three functions lay on top of each other. The finding that phase-reversal discrimination is *not* governed by the Fourier attributes of the stimulus *per se*, rules out an explanation in terms of a linear, broad-band, phase-sensitive mechanism. Rather, the results imply that information is combined across the set of SF- and orientation-tuned mechanisms before the decision variable. These interactions appear to be governed by the spatial (not Fourier) attributes of the luminance profile of the stimulus. A modified version of Bennett's [(1993) *Perception & Psychophysics, 53*, 292–304] phase discrimination model is presented as a *post-hoc* account of the data.

Psychophysics Phase discrimination Spatial frequency Spatial repetition Jitter

INTRODUCTION

Above threshold there is no doubt that the phase spectrum of a viewed scene is of considerable importance to the visual system (e.g. Piotrowski & Campbell, 1982). Several authors have considered the possibility that the visual system contains phase channels (Nachmias & Weber, 1975; Burr, 1980; Lawden, 1983; Field & Nachmias, 1984; Tyler & Gorea, 1986; Bennett & Banks, 1987; Burr, Morrone & Spinelli, 1989; Morrone, Burr & Spinelli, 1989; Bennett, 1993) as well as the well known orientation and spatial frequency channels (Campbell & Robson, 1968; Blakemore & Campbell, 1969; Movshon & Blakemore, 1973).

Lawden (1983) investigated the bandwidth of the putative phase channels by using one-dimensional (1-D), one- and two-component gratings, in both phase discrimination and compound detection experiments. The spatial frequency of one of the components of a compound grating (the base) was fixed at 1*F* and had a contrast fixed at 5%. The spatial frequency (SF) of the other component of the same compound grating (the test) was *nF*, defining the SF ratio (the ratio of the test SF to the base SF) as *n*. The contrast of the *nF* component was the independent variable in two different, three-alternative forced-choice (3AFC) tasks. In a compound detection task, the compound grating ($F + nF$) was discriminated from the base component (F) alone, and in a phase discrimination task, one compound grating ($F + nF$) was discriminated from a second compound grating, where the test component was phase reversed ($F - nF$). The phase relation between the base and the test was always either peaks-add or

*Department of Vision Sciences, Aston University, Birmingham B4 7ET, England.
†Present address: School of Psychology, Birmingham University, Edgbaston, Birmingham B15 2TT, England [*Email* t.s.meese@bham.ac.uk].

peaks-subtract and the SF ratio (n) was varied between $\frac{1}{6}$ and 6. Lawden expressed contrast thresholds for phase discrimination relative to those for compound detection and, independently of base SF, found a plateau, where phase discrimination thresholds were about half those for compound detection. The plateau extended from an SF ratio of about 1 to about 3.5. This superiority of phase discrimination over compound detection can be readily understood when the luminance profiles of the stimuli are considered. In the case of compound detection, there is a single luminance decrement (or increment) at the peak of the waveform in one interval. However, in phase discrimination, there is a luminance peak increment in one interval and a luminance peak decrement of the same magnitude in the other interval. Thus, the change in luminance is twice as large for phase discrimination as it is for compound detection. Lawden's (1983) results suggest that a comparison of these increments and decrements is available only for a limited range of SF ratios (Lawden, 1983): outside of the *phase-plateau*, the test components could be readily detected, but phase discrimination became increasingly difficult. For a SF ratio of 6, phase discrimination was impossible (Klein & Tyler, 1981; Lawden, 1983), though in similar experiments, Bennett (1993) found this limit to be somewhat higher for some of his observers and conditions.

Lawden interpreted his results in terms of phase-sensitive "patch" mechanisms that operate on the outputs of a limited range ($1F$–$3F$) of SF tuned channels. This is a Fourier account of the results because performance is dependent upon the *spatial frequency content* of the stimulus. However, in the next section I present a contrasting approach to early vision, and raise the possibility that the Fourier content of the stimulus *per se*, may not be what matters in phase reversal discrimination.

Fourier filters and perceived spatial structure

Typically, psychophysical models of spatial discrimination assume that the observer is able to make comparisons across a (limited) set of (linear) spatial filters, and that performance is determined by a limiting source of noise identified within the model (e.g. Wilson & Gelb, 1984). Indeed, after this noise stage, an arbitrary number of representations could exist before the decision variable, so long as they are noise free and information is not discarded. Models of this kind are sometimes referred to as error propagation models* (Bowne, 1990). Such models have little to say about explicit representations, and nothing to say about how neural activity maps onto our *perceptions* (see Shapley, Caelli, Grossberg, Morgan & Rentschler, 1990). In contrast, a different approach to early vision has recently been adopted by Georgeson and Meese (Georgeson, 1990, 1992, 1994; Meese & Georgeson, 1991, 1995; Georgeson & Meese, 1992; Meese & Freeman, 1995), who conducted a series of experiments investigating the perceived spatial structure of static plaid stimuli. For example, at moderate contrasts they found that a plaid with 1 c/deg components oriented at ± 45 deg, was perceived as a blurred checkerboard containing vertical and horizontal edges, though there is no Fourier energy at those orientations. Moreover, this perceived spatial structure is exactly the same as the spatially distributed pattern of zero-crossings (ZCs) in the stimulus.

These findings bring to mind the possibility that what matters in spatial discrimination tasks is the spatial distribution of features (e.g. edges) and not the spatial frequency content of the stimulus *per se*. For example, in Lawden's experiment, it could be that the spatial distribution of vertical ZCs (or their equivalent) in the filtered image (Yuille & Poggio, 1988) are what govern performance in phase-reversal discrimination. Of course, for 1-D gratings, the spatial frequencies of the constituent components are identical to the spatial repetitions of the component features. However, for two-dimensional (2-D) patterns these two attributes are decoupled. For example, a two-component plaid, with component orientations of $\pm\Theta$ deg from vertical, has a horizontal spatial repetition (SR) of $f_b \cdot \cos(\Theta)$, where f_b is the spatial frequency of the two plaid components. Figure 1 shows how the terms spatial frequency and (horizontal) spatial repetition apply to a grating (a) and a plaid whose components are at ± 45 deg (b). Note that the SR of the plaid is lower than the SR of the grating (by half an octave), though the constituent components of the plaid have the same spatial frequency as that of the grating.

Suppose that a vertical test component is now superimposed on each of the two base patterns shown in Fig. 1. The ratio of the test SR to the base SR defines the (horizontal) SR ratio for each of the resulting compound patterns, and is less for the plaid than it is for the grating. However, the SF ratio (test SF: base SF) for the grating and plaid compound patterns is the same.

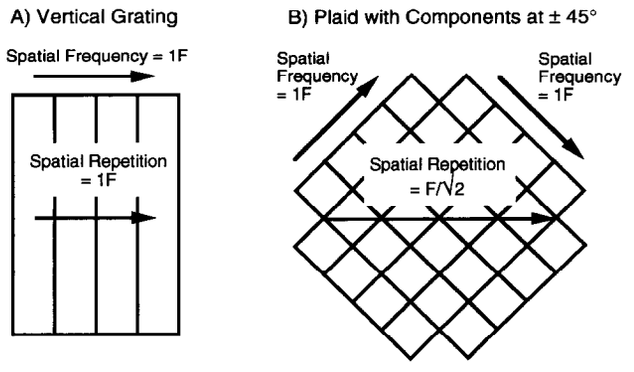

FIGURE 1. Spatial structure of base patterns. Relation between spatial frequency and spatial repetition in a vertical grating (A) and a two-component plaid whose components are at $\pm\Theta$ (B). Formally, the horizontal spatial repetition of a Fourier component is given by its U coordinate in the Fourier domain, where $U = F \cdot \cos(\Theta)$, F is the spatial frequency and Θ is the orientation of the Fourier component. Thus, for both (A) and (B), spatial frequency is given by F in the Fourier domain, and spatial repetition is given by U in the Fourier domain.

*Morgan has referred to these theories as "primal soup" models (Shapely *et al.*, 1990), in stark contrast to primal sketch models (Marr, 1982; Watt & Morgan, 1985), where spatial primitives are made explicit.

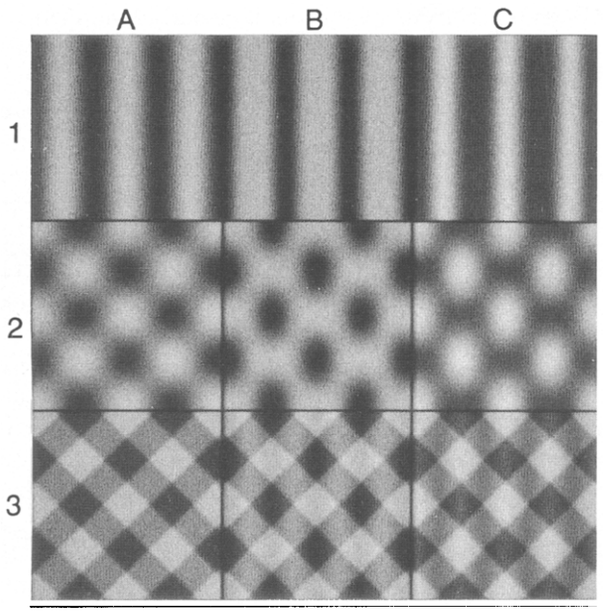

FIGURE 2. High contrast examples of some of the stimuli used in the experiments. Different rows show the grating condition (row 1), the sine-plaid condition (row 2) and the SqW-plaid condition (row 3). (A) 1*F* base patterns with no test components added. (B, C) 1*F* base patterns with vertical test components in peaks-subtract phase and peaks-add phase respectively. The spatial frequency of the test component is twice the horizontal spatial repetition of the base pattern. In the compound detection task, observers discriminated between patterns like those in columns (A) and (B). In the phase discrimination task, observers discriminated between patterns like those in columns (C) and (B). Note that second harmonic distortion caused by the reproduction process may have introduced a vertical 2*F* component in pattern 1(A), magnified the 2*F* component in pattern 1(B) and nulled the 2*F* component in pattern 1(C). The consequence of this is that patterns 1(A) and 1(C) may appear to have been transposed. The linearity of the display ensured that this type of stimulus distortion did not occur in the experiment.

The purpose of the work reported here was to discover whether the phase-reversal discrimination functions found by Lawden are indeed dependent on the SF ratio as suggested by Lawden (1983), or instead, upon the SR ratio as suggested here. It is only if the first hypothesis is supported, that experiments of the type performed by Lawden (1983) can be viewed as providing information about the bandwidth of phase-sensitive mechanisms.

Experimental rationale

To decide between the two hypotheses, compound detection and phase discrimination experiments similar to those performed by Lawden (1983) were carried out using three conditions (see Fig. 2). In the first condition, a vertical 1 c/deg grating (1*F*) was used as the base pattern (grating condition). In the second condition (sine-plaid condition), the base pattern was made from sine-wave components at orientations of ± 45 deg and spatial frequencies of 1 c/deg (1*F*). In the third condition (SqW-plaid condition), the two gratings comprising the base pattern were square-waves instead of sine-waves. For all conditions, the test component was a vertical grating of spatial frequency *nF*. Thus, for a given value of *n*, the SF ratio for each of the three conditions is the same, but the SR ratio for each of the two plaid conditions is half an octave higher than the grating condition (see Fig. 1).

The idea is that the results from the grating condition provide a *signature* for performance in phase discrimination relative to that in compound detection: the function is identical whether plotted against SF ratio or SR ratio. By comparing this signature with the plaid results plotted against both SF ratio and SR ratio, it should be possible to establish which of these two ratios determines the placement of the phase-plateau and the absolute limit for phase discrimination (i.e. the point at which phase discrimination becomes impossible). *This was the main reason for conducting the experiments.* However, the SqW-plaid condition was included to investigate a secondary hypothesis as follows:

Is perceptual integration important in phase discrimination?

In both 1-D (Thomas, 1989; Georgeson, 1990) and 2-D (Georgeson, 1990), two-component stimuli are perceived as a single compound structure so long as the SF ratio is low, while at higher SF ratios, the stimulus is perceived as two overlapping gratings. For example, in 1-D, perceptual combination of components appears to take place between SF ratios of 1 and about 3.5. This is about the same as the upper extent of the phase-plateau found by Lawden. Bennett (1993) also remarked that perceptual integration may be important in phase discrimination. Taken together, these results hint that optimal phase coding may require that Fourier components are perceived as a single compound structure. One way to investigate this possibility is to compare the performance in two conditions where the fundamental base components are matched, but where perceptual integration occurs for only one of them. The two plaid conditions provide this comparison: for the stimuli in the SqW-plaid condition, the vertical test grating is never perceptually integrated into the pattern, while for the sine-plaid condition, there is a range if SF ratios were perceptual integration occurs. This categorical difference is readily seen in Fig. 2. For example, the only difference between the stimuli in rows 2 and 3 is the presence of the oblique square-wave harmonics: in their absence [Figs 2.2 (B, C)], the vertical test grating is perceptually integrated into the base pattern, while in their presence [Fig. 2.3 (B, C)], it is not. This observation is compatible with the edge-coding model presented by Georgeson (1992), where, prior to the extraction of ZCs, the outputs of spatial filters are *selectively* combined across ranges of both orientation and spatial frequency. For example, in two-component plaids at 1 c/deg, perceptual combination *across* orientation (blurred checkerboard percept) is changed to perceptual combination *within* orientation and across spatial scales (tessellating diamonds percept), when square-wave harmonics are added at either one or both of the orientations of the original plaid components (Georgeson, 1990, 1994; Meese, 1993).

So, the SqW-plaid condition was included to discover whether perceptual integration is necessary for optimum phase-discrimination.

METHODS

Equipment and subjects

Stimuli were generated using an Inisfree Picasso Image Synthesizer with a frame rate of 242 Hz under the experimental control of an Acorn Archimedes 440 computer and displayed on a Tektronix 608 oscilloscope with green phosphor (P31). The stimulus components (either square-wave or sine-wave) were produced by modulating the z-axis of the oscilloscope, and plaids and complex gratings were generated by temporally interleaving the components, which could be rotated by changing the direction of the raster scan between frames. The software took two frames to calculate the rotation and instruct the hardware, giving a picture refresh rate for three-component stimuli of 40 Hz. So that the picture refresh rate was identical for all conditions, the fundamental component of two-component gratings was treated as two components having the same phase, orientation and spatial frequency, but each having only half of the required amplitude.

The display field was circular with a black surround and had a mean luminance of 17 cd/m^2. Routine calibration of the contrast and luminance linearity of the display was performed using a Photodyne digital photometer (model 88XLA). The display was found to be linear and stable up to a contrast of 40%. The contrast levels used in the experiment were well within this useful operating range.

Subjects viewed the display binocularly with natural pupils and the aid of a chin and forehead rest in a darkened room and had normal or corrected to normal vision. Subjects were instructed to fixate a small dot at the centre of the screen during stimulus presentations.

In order to accommodate the required SF range, while also maximizing the number of cycles per screen for conditions that employed low SFs, some sessions were performed at a viewing distance of 228 cm with a field diameter of 2.5 deg, while others were performed at a viewing distance of 114 cm with a field diameter of 5 deg.

Stimuli

All stimuli consisted of a base pattern plus a test component in three different conditions (see Fig. 2). The base pattern was either a vertical grating of 16% contrast (grating condition); a plaid with sinusoidal components at ± 45 deg and component contrasts of 8% (sine-plaid condition); or a plaid with square-wave components at ± 45 deg (SqW-plaid condition), where the fundamental components were matched in contrast to those in the sine-plaid condition (i.e. the Michelson contrast of a single square-wave component of the SqW-plaid was $\pi/4$ times that of a single sinusoidal component in the sine-plaid). The SF of the fundamental components in each of the three conditions was either 1 c/deg (Expt 1) or 2 c/deg (Expt 2).

The test component was always a vertical grating and was summed in either peaks-add phase or peaks-subtract phase with the base pattern. The SF of the test component was either a multiple of the horizontal SR of the base pattern in the range 1–10, or two-thirds of this SR, or one-third of this SR.* The contrast of the test component was controled by a staircase procedure (see below).

Example stimuli are shown in Fig. 2 for the grating condition (row 1), the sine-plaid condition (row 2) and the SqW-plaid condition (row 3). In column A, the test component has 0% contrast. In column B, the test component is in peaks-subtract phase with the base pattern and in column C, the test and base are in peaks-add phase. The SR ratio for the stimuli in the second two columns is 2. In other words, the horizontal SR of the test component is twice that of the base pattern. Note that because all of the base components of the stimuli in Fig. 2 have the same spatial frequency ($1F$), an SR ratio of 2 is achieved by using a test SF of $2F$ in the grating condition (row 1) and a test SF of $1.414F$ in the two plaid conditions (rows 2 and 3).

The lateral phase of the whole stimulus relative to the fixation point (i.e. the horizontal position of the stimulus) was randomized from trial to trial so as to remove local luminance cues.

Procedure

A two-interval forced-choice (2IFC) technique with a randomly interleaved double staircase (Cornsweet, 1962), configured to converge on the 79.4% correct point of the psychometric function (Wetherill & Levitt, 1965), was used to drive the contrast level of the test component. Contrast is given in dB units and is equal to $20 \cdot \log_{10}(C)$, where C is Michelson contrast in percent. The initial step-size of a *leading staircase* was set to 8 dB. This was reduced to 4 dB after the first reversal and then 2 dB after the second reversal where it remained for a further seven reversals. The initial stimulus level for this staircase was set well above the estimated compound detection threshold. A second, *companion staircase*, had an initial step size of 2 dB and started at the contrast level recorded at the third reversal of the leading staircase. The companion staircase terminated after six reversals and the whole procedure typically terminated after 60–80 trials. The data collected at and beyond the fourth reversal of the leading staircase, and the first reversal of the companion staircase, were collapsed, and thresholds were taken to be the 75% correct point determined by probit analyses. In cases where probit analyses could not be performed, linear interpolation was used instead. In cases where there was ambiguity over where to perform this interpolation, the data were discarded (see below).

Stimulus duration was 200 msec and the duration between the two stimulus intervals was 1250 msec. In a phase discrimination task, one interval contained the stimulus in peaks-subtract phase while the other

*It was not possible to perform the experiment with the test grating at one-half of the SR of the base pattern because phase inversion of the test grating would have been indiscriminable from the lateral translation of the stimulus which was employed to control for local luminance cues.

contained it in peaks-add phase [see Fig. 2 (B, C)]. In a compound detection task one interval contained the stimulus in peaks-subtract phase, while the other contained only the base component: the test component was set to 0% [see Fig. 2 (A, B)].* For each task, the interval order was random and the observer's task was always to select the interval that contained the test component in peaks-subtract phase with the base pattern. This was done by pressing one of two response buttons. Correctness of the response was indicated by auditory feedback. Each session always started with several moderately high contrast dummy trials so that the observer was able to establish the response cues. The observer was free to proceed with this preliminary stage for as long as he wished, though in practice only two or three trials were usually required. However, in order to avoid contamination by learning effects (Fiorentini & Berardi, 1981; Badcock, 1984a; Kiper, 1994), experimental sessions did not commence until performance in practice sessions appeared to be optimum.

In Expt 1, where TSM (the author) served as the subject, staircase pairs measuring compound detection and phase discrimination were randomly interleaved (four staircases in all) and a visual cue to the task type was presented on a display monitor in the observer's periphery. However, in Expt 2, where a naive observer (TCAF) was used, this interleaving of tasks was abandoned in order that the task requirements were not too difficult to learn. Instead, for each sesson, the compound detection and phase discrimination tasks were performed contiguously in a random order.

Experimental sessions were performed in three (for TSM) or four (for TCAF) blocks of conditions in a pseudo random order. In cases where neither probit analyses nor linear interpolation could be performed, and cases where the leading and companion staircases converged on thresholds that were more than 8 dB apart, data were discarded and the sessions were rerun.

RESULTS

Experiment 1

In Fig. 3, phase discrimination thresholds are plotted relative to compound detection thresholds as a function of SF ratio for both grating (●) and sine-plaid (□) base patterns.

Of some concern was the rather mysterious "blip" in the data for the sine-plaid condition at an SF ratio of 4.26. Inspection of the individual functions for phase discrimination and compound detection (not shown) indicated that the blip has its origin in the phase discrimination data. To further investigate, eight additional sessions of phase discrimination and compound detection were performed for the sine-plaid condition with a test component of 4.24 c/deg. For the compound detection task, mean threshold was −6.173 dB (SE = 0.49) and compares favourably with a mean threshold of −6.94 dB (SE = 0.73) found in the main experiment. However, for phase discrimination, mean threshold was −9.37 dB (SE = 0.65) and is considerably higher than the threshold of −16.2 dB (SE = 0.43) found in the main experiment. As there is no obvious reason for this difference, the second measurement probably better represents the true phase discrimination threshold for this condition because it was derived from a greater number of replications.

The two data sets shown in Fig. 3 share several similarities. For example, both conditions have a broad region where phase discrimination thresholds are about half of the corresponding compound detection thresholds (indicated by the horizontal dashed line). However, although the shapes of the two functions are similar, they are not superimposed, but instead, appear to be lateral translations of each other. Crucially, however, when the same data are plotted as a function of SR ratio as in Fig. 4, they are clearly more alike. For example, in this figure, both the phase plateau, and the limit for phase discrimination are aligned, whereas in Fig. 3 they were not.

Figure 5 shows the results from the SqW-plaid condition (◇), alongside those from the sine-plaid condition (□) and the grating condition (●) as a function of SR ratio. The ■ indicates the repeated measure for the sine-plaid condition reported earlier in this section. All three data sets have a qualitatively similar form, supporting the idea that it is the spatial repetition of the stimulus that governs the breadth and placement of the phase-plateau. The two curves in this figure (solid and dashed) illustrate variations of a model proposed by Bennett (1993), and are described in the Discussion and the Appendix.

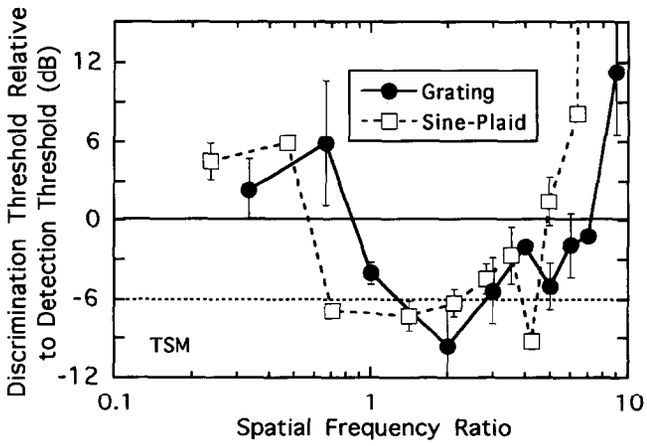

FIGURE 3. Phase discrimination thresholds relative to compound detection thresholds for the sine-plaid condition (□) and the grating condition (●). Symbols and error bars show the means and ±1 SE of three different measures. The solid horizontal line shows the level where phase discrimination performance is equal to that in compound detection. The dashed horizontal line shows the level at which phase discrimination thresholds are half of the compound detection thresholds. The data are plotted as a function of the ratio of the test SF to the SF of the base pattern. The SF of the base pattern was 1 c/deg.

*Lawden (1983) and Bennett (1993) found practically no difference between peaks-add and peaks-subtract conditions in compound detection across a wide range of SF ratios for two-component gratings.

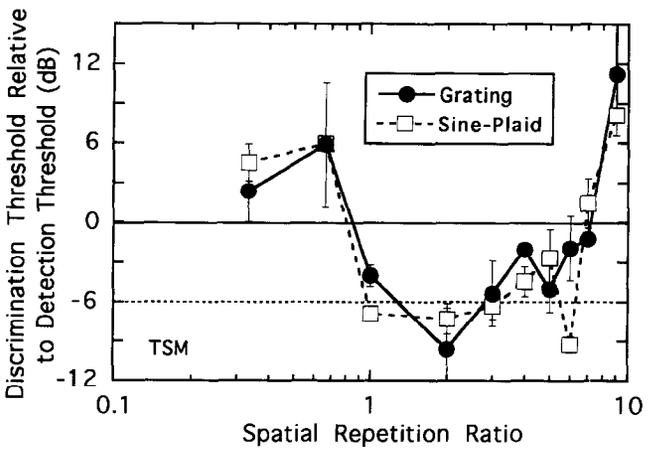

FIGURE 4. The same data as shown in Fig. 3, but instead plotted as a function of SR ratio.

Performance in the SqW-plaid condition (Fig. 5) was impressive: at high SR ratios, discrimination was better in this condition than it was in either of the other two conditions. This rules out the hypothesis that perceptual integration is required for optimal performance in *phase-reversal discrimination*, because perceptual integration does not occur for the SqW-plaid condition (see Introduction). Consequently, this hypothesis will not receive further consideration.

Experiment 2

Experiment 2 was similar to Expt 1 and was performed primarily to collect data from a naive observer. In order to minimize the duration of data collection, the SqW-plaid condition was omitted and data were gathered only for three SR ratios at a single end of the phase-plateau (low SR ratios). A second modification was to increase the fundamental SF of the base pattern

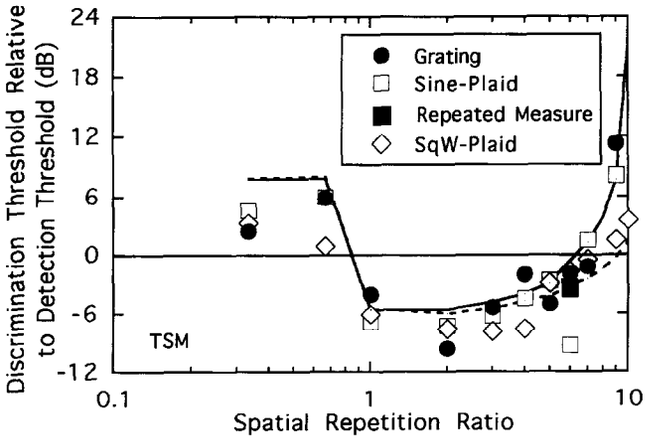

FIGURE 5. The same as Fig. 4 but with the addition of a repeated measure ($n = 8$) for the sine-plaid condition (■) and the results from the SqW-plaid condition (◇). Standard error bars have been omitted for clarity. Model curves are for independent positional jitter of two components (dashed curve) and 100% correlated component jitter (solid curve). The single free parameter of the model is the standard deviation of the Gaussian positional jitter applied to the process that localizes the test pattern and was set to 10 deg of base phase angle to provide a good fit by eye. See Discussion and Appendix for model details.

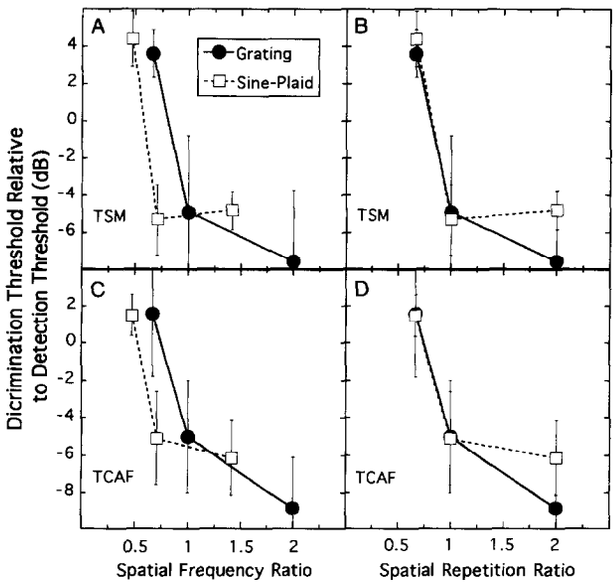

FIGURE 6. Phase discrimination thresholds relative to compound detection thresholds for TSM (A, B) and a naive observer TCAF (C, D). Data are for a grating base pattern (●) and a sine-plaid base pattern (□). In (A, C) the results are plotted as a function of SF ratio, and in (B, D) the results are plotted as a function of SR ratio. The SF of the base pattern was 2 c/deg.

from 1 to 2 c/deg. There were two reasons for this. The first was to demonstrate that the results from Expt 1 were not specific to a single base SF. The second was to increase the minimum number of test cycles in the display to 4.66 in order to ensure that performance was not limited by a shortage of test cycles.

Figure 6 shows phase discrimination thresholds relative to compound detection thresholds, as a function of SF ratio [Fig. 6 (A, C)], for two different observers. For both observers, the results for the sine-plaid condition (□) appear to be a leftward translation of the results for the grating condition (●). Figure 6 (B, D) show the same results replotted as a function of SR ratio, and like those of Expt 1, are now superimposed.

DISCUSSION

Phase-reversal discrimination is dependent upon spatial repetition

There are two aspects of the experimental results reported here that support the idea that it is the SR of the base pattern and not its spatial frequency content that limits performance in a phase-reversal discrimination task. First, the absolute limit for phase discrimination in Expt 1 is at a common SR ratio for the grating and sine-plaid conditions (SR ratio = 9, see Fig. 4), rather than a common SF ratio. Second, for both Expts 1 and 2, the placing of the phase-plateau is determined by the SR ratio and not the SF ratio. If the reasonable assumption is made that both the 1-D and the 2-D results owe their explanations to a common general processing scheme, then these results rule out an explanation of phase-reversal discrimination in terms of a linear, broad-band, phase-sensitive mechanism (Nachmias & Weber, 1975; Burr, 1980; Lawden, 1983;

Field & Nachmias, 1984). This is because sine-plaid base patterns contain no Fourier energy at their SR, and so no linear filter would be sensitive to the spatial repetitions of those patterns in the way indicated in Figs 4, 5 and 6.

Can the results reported here be understood in terms of any other types of phase discrimination model?

Nielsen, Watson and Ahumada (1985), developed Watson's (1983) template matching model by adding positional uncertainty and showed that the results from several classes of phase discrimination experiments (Nachmias & Weber, 1975; Burr, 1980; Lawden, 1983) could be understood without the need to employ phase-labelled channels. However, their original model was not able to account for the precipitous role-off in performance at high SF ratios in phase-reversal discrimination. A further modification assumed information to be available only from neighbouring pairs of spectrally adjacent spatial frequency channels, allowing the model to describe performance at high SF ratios. However, even with the assumption of limited communication between SF channels, it is likely that Nielsen *et al.*'s model would predict that phase-reversal discrimination would be limited by SF ratio and not SR ratio. This is because in their model, the role-off in performance is determined by the range of SF tuned filters that are available for the discrimination, rather than some characteristic of the stimulus.

Hoffman and Hallett (1993b) modelled early cortical physiology and showed that by pooling information across orientation (and in principal, spatial frequency), they were able to account for certain preattentive phase discrimination results in 2-D (e.g. Hoffman & Hallett, 1993a). Unfortunately, the inclusion of logistic response nonlinearities both before and after interactions between oriented filters make it difficult to predict how their model would perform in the phase discrimination task used here: performance would depend on the effective bandwidth of the overall filter after pooling, though whether the nonlinear interactions would produce a filter whose bandwidth depends on the SR of the stimulus requires detailed modelling.

An overview of the remainder of the paper

I attribute the role-off in phase-reversal discrimination performance at high SF ratios to positional jitter in the representation of the base pattern and explain the data with a modified version of a model first presented by Bennett (1993). However, in order to account for the similarity between the sine-plaid results and the grating results at high SR ratios, the jitter for each of the two base components must be 100% correlated. One way in which this could be so is to assign this limiting source of noise to the output of a single mechanism. Recent studies on the perceived spatial structure of static plaids (e.g. Georgeson, 1992; Meese & Georgeson, 1995), suggests that this mechanism is best viewed as a combination of oriented filters rather than as a circular filter (e.g. Marr & Hildreth, 1980).

Bennett's (1993) model of phase-reversal discrimination

One useful framework for understanding the results reported here was provided by Bennett (1993), who described his own phase-reversal discrimination data using a model that employed spatial positional jitter. In order to understand the working of the modified model used here, first consider only the grating condition (full details are presented in the Appendix). Compound detection and, at moderate SF ratios, phase discrimination, are limited by independent Gaussian noise added to the outputs of cosine-phase test filters that, like Bennett (1993), are assumed to respond only to the test component. In compound detection, the placement of these filters is irrelevant, but in phase discrimination, a peak in the base pattern is used to identify the test filters that are to be used for the discrimination.

For each of the two experimental intervals, the test filters are identified independently and a comparison of their outputs is made: the interval containing the smaller signed response is the one in which the components are in peaks-subtract phase.* However, the identification process is perturbed by a further source of Gaussian noise which introduces positional jitter and ultimately limits performance at high SF ratios. The standard deviation of this jitter is the model's only free parameter, and in Fig. 5 (solid curve) was set to 10 deg of base phase-angle for the grating condition, in order to provide a reasonable fit by eye. The model provides a particularly good account of the role-off in performance at high SF ratios.

Unlike the present study, Bennett (1993) considered only conditions where the test pattern was harmonically related to the base pattern and where SF ratios were >2. This means that some thought has to be given to the model's implementation at low, noninteger SF ratios, because in those cases, the activity expected in the test filters is not the same for each peak in the base pattern and so the choice of base peak becomes important. The solution proposed here was to monitor the test filter outputs localised by three neighbouring peaks of the base component. The details of this process and the modifications to the decision rules are outlined in the Appendix.

The model shown in Fig. 5 captures the overall form of the data quite well, though there is a tendency for the model to underestimate performance at low SR ratios, where the decision rules were *post hoc*. On the other hand, no serious attempt was made to optimize the way in which information is combined from neighbouring peaks in the base pattern (i.e. an ideal observer was not assumed). Alternatively, a model based on local contrast at low SR ratios (Hess & Pointer, 1987; Field, 1984) may be more appropriate. To address this issue in detail, more experiments are required, but the important point here is that if the response strategy does change when the

*Note that an alternative response strategy that simply chooses the interval containing the negative response would be inferior to the one used here because when the filter responses are subjected to noise, both (or neither) of the filter responses could be negative.

SF of the test component is reduced (Hess & Pointer, 1987), the change is critical on the SR ratio and not the SF ratio.

Phase discrimination in 2-D

Although Bennett (1993) does not state it explicitly, one interpretation of the localization process is a search for a local maximum in a spatial array of oriented cosine-phase filters tuned to the base SF. The spatial positional jitter used in his model is an indication of the fidelity of this process and could summarize several sources of noise including, local jitter in contrast response and uncertainty of the spatial position (local sign) of the most active base filter once it is identified. This means that if the noise that limits the localization process occurs at the filter output level, then the positional jitter would be independent for each component of the base pattern in the sine-plaid condition used here. This is illustrated by the dashed curve in Fig. 5, where the independent component jitter is set equal to that in the grating condition (see the Appendix). The model clearly predicts performance to be better than that found behaviourally at high SR ratios (cf. dashed curve with sine-plaid data at SR ratios of 7 and 9 in Fig. 5).

100% correlated component jitter

The experimental results show that the role-off in phase discrimination performance is not determined by the spatial frequency content of the stimulus, but rather, its spatial repetition. This is equivalent to assuming 100% correlated jitter between the two components of the base pattern. With this important modification, the model curves for the grating condition and the sine-plaid condition are identical when plotted as a function of SR ratio (see Appendix and the solid curve in Fig. 5).*

Two possible interpretations of the 100% correlated jitter are (i) the localization process (i.e. the limiting noise) is applied after the outputs of a single array of filters that are sensitive to both base components [e.g. circular filters (Marr & Hildreth, 1980; Hildreth, 1983; Watt, 1988)], or (ii) the process is applied after a stage where filters that are tuned to the individual components of the base pattern are combined (Georgeson, 1992). The important point is that in either case, the jitter can be viewed as a single source of noise that characterises positional uncertainty *after* the representation of the combined response distribution for the base pattern, and is related to, for example, the horizontal spacing of features (e.g. filtered luminance edges or peaks).

Under this interpretation, it would be expected that if the location of the useful features were made more precise, e.g. by increasing their sharpness (Watt & Morgan, 1983; Georgeson & Freeman, 1993; Georgeson, 1994), then performance should improve, because positional jitter would be reduced. This is exactly what was found in the SqW-plaid condition where it was still possible to perform phase-reversal discrimination at the highest SR ratio tested, while this was not so for either the grating condition or the sine-plaid condition (see Fig. 5). Indeed, Fig. 2 illustrates that in the SqW-plaid condition (row 3), the horizontal coordinate of the centre of the base pattern is clearly marked by the points of upward and downward pointing chevrons and Westheimer and McKee (1977) have demonstrated that the point of a line drawing of a chevron can be accurately localised in a hyperacuity task.

Finally, near 100% correlated noise has also been found across disparate frequency bands [3 and 15 c/deg (Olzak, Wickens & Thomas, 1994)], in an orientation discrimination task were the two components were at nearly the same orientation.

Circular filters or the combination of oriented filters?

Although this study is not able to distinguish between the use of circular base filters (Marr & Hildreth, 1980; Watt, 1988) or the combination of oriented base filters (Georgeson, 1992), there are good grounds for preferring the latter over the former. Georgeson (1992) and Meese and Georgeson (1995) found that after selective adaptation, the perceived spatial structure of suprathreshold, two-component plaids became perceptually distorted. This distortion could not be understood by considering the outputs of circular filters (Marr & Hildreth, 1980; Hildreth, 1983; Watt, 1988), but rather, implied that the outputs of oriented filters (Campbell & Kulikowski, 1966; Movshon & Blakemore, 1973; Phillips & Wilson, 1984; Snowden, 1992) can be combined across orientation prior to edge-coding. This scheme sits comfortably with the findings that component processing in static two-component plaids is not independent in a component orientation discrimination task (Olzak & Thomas, 1992).

Shortcomings and interpretations of the model

One shortcoming of the model is that, like Bennett (1993), it is assumed that the test filters respond only to the test components. This will not always be the case.

*An alternative, but less parsimonious interpretation is possible, whereby the positional jitter remains independent for each component of the sine-plaid base pattern. Consider first, the independent component model indicated by the dashed curve in Fig. 5. An implicit assumption is that the localization process for each component integrates along the length of the component and assigns a position for the whole component based upon this response. For each base component (j), the positional jitter in the direction orthogonal to its orientation is given by $G_j(\sigma_s)/f_b$, where f_b is the spatial frequency of the base component and $G_j(\sigma_s)$ denotes a Gaussian random variable with a standard deviation of σ_s. Thus, after positional jitter, the locations of peaks in each sinusoidal base component are given by loci that form lines at the same orientations as each of the base components. The *horizontal* position of each of these lines is given by $x + G_j(\sigma_s)/f_b \cdot \cos(\Theta)$, where Θ is the orientation of each of the base component's and x is the true horizontal spatial coordinate of a component's peak for any given vertical coordinate. The locations of peak responses to a base pattern made from two sinusoidal components are given by the intersections of lines. This is the independent component model. However, if it is further assumed that the identification of the intersection of the two components is also subject to noise and that, critically, for the conditions in Expt 1, the standard deviation of that noise is $\sigma_s \cdot \sqrt{(\frac{3}{2})}$, then the independent component model is also given by the solid line in Fig. 5.

For example, in the grating condition, when the SF ratio is unity, both the base component and the test component must be seen by the same filter, because the two components have the same orientation and spatial frequency. In such a case, the effects of response compression observed above threshold (Legge, 1981; Wilson, 1980; Legge & Foley, 1980; Georgeson, 1991), would be to produce data that are slightly inferior to model predictions (see the grating condition in Fig. 5 at a SR ratio of 1).

In general, this model, like many conventional psychophysical models, employs a decision variable that is computed by accessing directly the outputs of a bank of front-end spatial filters (e.g. Sachs, Nachmias & Robson, 1971; Legge & Foley, 1980; Wilson, McFarlane & Phillips, 1983). However, other interpretations of the model are not ruled out. For example, the use of cosine-phase filters in the discrimination stage means that this model is compatible with a scheme that generates a symbolic description of the viewed scene in terms of edges represented by zero-crossings (Marr & Hildreth, 1980) after combining the outputs of spatial filters (Georgeson, 1992; Meese, 1993). Indeed, there is a growing body of work suggesting that observers are unable to make direct access to the outputs of spatial filters, but that in perception and discrimination, the decision variables arise at a later stage in processing (Burbeck, 1987; Bowne, 1990; Olzak & Thomas, 1991, 1992; Nachmias, 1993; Olzak *et al.*, 1994). One implication drawn here, that component jitter in the base pattern is 100% correlated, also supports this view.

CONCLUSIONS

It has been shown that phase-reversal discrimination cannot be understood in terms of a linear, broadband, phase-sensitive mechanism (Nachmias & Weber, 1975). Rather, because it is the spatial repetition and not the spatial frequency of a base pattern that limits performance at high SF ratios, the implication is that the limiting source of noise comes after the coding of spatial repetition (e.g. feature extraction). It remains to be seen whether phase-angle discrimination (Burr, 1980; Badcock, 1983a, b), and spatial frequency discrimination (Wilson & Gelb, 1984; Bowne, 1990), are also better viewed in terms of spatial repetition rather than spatial frequency.

REFERENCES

Badcock, D. R. (1984a). Spatial phase or luminance profile discrimination? *Vision Research, 24*, 613–623.

Badcock, D. R. (1984b). How do we discriminate spatial phase? *Vision Research, 24*, 1847–1857.

Bennett, P. J. (1993). The harmonic bandwidth of phase-reversal discrimination. *Perception & Psychophysics, 53*, 292–304.

Bennett, P. J. & Banks, M. S. (1987). Sensitivity loss in odd-symmetric mechanisms and phase anomalies in peripheral vision. *Nature, 326*, 873–876.

Blakemore, C. & Campbell, F. W. (1969). On the existence of neurones in the human visual system selectively sensitive to the orientation and size of retinal images. *Journal of Physiology, 203*, 237–260.

Bowne, S. F. (1990) Contrast discrimination cannot explain spatial frequency, orientation or temporal frequency discrimination. *Vision Research, 30*, 449–461.

Burbeck, C. A. (1987). Locus of spatial-frequency discrimination. *Journal of the Optical Society of America A, 4*, 1807–1813.

Burr, D. C. (1980). Sensitivity to spatial phase. *Vision Research, 20*, 391–396.

Burr, D. C., Morrone, M. C. & Spinelli, D. (1989). Evidence for edge and bar detectors in human vision. *Vision Research, 29*, 419–431.

Campbell, F. W. & Kulikowski, J. J. (1966). Orientation selectivity of the human visual system. *Journal of Physiology, 187*, 437–445.

Campbell, F. W. & Robson, J. G. (1968). Application of Fourier analysis to the visibility of gratings. *Journal of Physiology, 197*, 551–566.

Cornsweet, T. N. (1962). The staircase-method in psychophysics. *American Journal of Psychology, 75*, 485–491.

Field, D. J. (1984). A space domain approach to pattern vision: An investigation of phase discrimination and masking. Ph.D. thesis, University of Pennsylvania, Philadelphia, Pa.

Field, D. J. & Nachmias, J. (1984). Phase reversal discrimination. *Vision Research, 24*, 341–345.

Fiorentini, A. & Berardi, N. (1981). Learning in grating waveform discrimination: Specificity for orientation and spatial frequency. *Vision Research, 21*, 1149–1158.

Georgeson, M. A. (1990). Human vision combines oriented filters to compute edges. *Perception, 19*, 354.

Georgeson, M. A. (1991). Contrast overconstancy. *Journal of the Optical Society of America A, 8*, 579–586.

Georgeson, M. A. (1992). Human vision combines oriented filters to compute edges. *Proceedings of the Royal Society of London B, 240*, 235–245.

Georgeson, M. A. (1994). From filters to features: Location, orientation, contrast and blur. In *Higher order processing in the visual system (Ciba Foundation Symposium 184)* (pp. 147–165). Chichester: Wiley.

Georgeson, M. A. & Freeman, T. C. A. (1993). Perceived edge blur in one-dimensional and two-dimensional images. *Perception (Suppl.), 22*, 21.

Georgeson, M. A. & Meese, T. S. (1992). The tilt aftereffect in a two-dimensional stimulus: Image reconstruction takes place before edge extraction. *Perception (Suppl. 2), 21*, 6.

Hess, R. F. & Pointer, J. S. (1987). Evidence for spatially local computations underlying discrimination of periodic patterns in fovea and periphery. *Vision Research, 27*, 1343–1360.

Hildreth, E. C. (1983). The detection of intensity changes by computer and biological vision systems. *Computer Vision, Graphics and Image Processing, 22*, 1–27.

Hoffman, M. I. & Hallett, P. E. (1993a). Texture segregation based on two-dimensional relative phase differences in composite sine-wave grating patterns. *Vision Research, 33*, 221–234.

Hoffman, M. I. & Hallett, P. E. (1993b). Preattentive discrimination of relative phase modelled by interacting Gabor or by difference of Gaussian filters. *Vision Research, 33*, 2569–2587.

Kiper, D. C. (1994). Spatial phase discrimination in monkeys with experimental strabismus. *Vision Research, 34*, 437–447.

Klein, S. A. & Tyler, C. W. (1981). Phase discrimination using single and compound gratings. *Investigative Ophthalmology and Visual Science (Suppl.), 20*, 134.

Lawden, M. C. (1983). An investigation of the ability of the human visual system to encode spatial phase relationships. *Vision Research, 21*, 457–467.

Legge, G. E. (1981). A power law for contrast discrimination. *Vision Research, 21*, 457–467.

Legge, G. E. & Foley, J. M. (1980). Contrast masking in human vision. *Journal of the Optical Society of America A, 70*, 1458–1464.

Marr, D. (1982). *Vision*. San Francisco, Calif.: Freeman.

Marr, D. & Hildreth, E. (1980). Theory of edge detection. *Proceedings of the Royal Society of London B, 207*, 187–217.

Meese, T. S. (1993). Feature coding in human pattern vision. Ph.D. thesis, University of Bristol, Bristol.

Meese, T. S. & Freeman, T. C. A. (1995). Edge computation in human vision: Anisotropy in the combining of oriented filters. *Perception*. In press.

Meese, T. S. & Georgeson, M. A. (1991). Edge computation in human vision: What controls the combining of oriented filters? *Perception, 20*, 81.

Meese, T. S. & Georgeson, M. A. (1995). The tilt aftereffect in plaids and gratings: Channel codes, local signs and 'patchwise' transforms. *Vision Research*. Submitted.

Morrone, M. C., Burr, D. C. & Spinelli, D. (1989). Discrimination of spatial phase in central and peripheral vision. *Vision Research, 29*, 433–445.

Movshon, J. A. & Blakemore, C. (1973). Orientation specificity and spatial selectivity in human vision. *Perception, 2*, 53–60.

Nachmias, J. (1993). Masked detection of gratings: The standard model revisited. *Vision Research, 33*, 1359–1366.

Nachmias, J. & Weber, A. (1975). Discrimination of simple and complex gratings. *Vision Research, 15*, 217–223.

Nielson, K. R. K., Watson, A. B. & Ahumada, A. J. Jr (1985). Application of a computable model of human spatial vision to phase discrimination. *Journal of the Optical Society of America A, 2*, 1600–1606.

Olzak, L. A. & Thomas, J. P. (1991). When orthogonal orientations are not processed independently. *Vision Research, 31*, 51–57.

Olzak, L. A. & Thomas, J. P. (1992). Configural effects constrain Fourier models of pattern discrimination. *Vision Research, 32*, 1885–1898.

Olzak, L. A., Wickens, T. D. & Thomas, J. P. (1994). Higher-level edge detectors mediate complex orientation discriminations. *Perception (Suppl.), 23*, 2.

Phillips, G. C. & Wilson, H. R. (1984). Orientation bandwidths of spatial mechanisms measured by masking. *Journal of the Optical Society of America A, 1*, 226–232.

Piotrowski, L. N. & Campbell, F. W. (1982). A demonstration of the visual importance and flexibility of spatial-frequency, amplitude and phase. *Perception, 11*, 337–346.

Press, W. H., Flannery, B. P., Teukolsky, S. A. & Vetterling, W. T. (1989). *Numerical recipes in Pascal: The art of scientific computing*. Cambridge: Cambridge University Press.

Sachs, M. B., Nachmias, J. & Robson, J. G. (1971). Spatial-frequency channels in human vision. *Journal of the Optical Society of America, 61*, 1176–1186.

Shapely, R., Caelli, T., Grossberg, S., Morgan, M. & Rentschler, I. (1990). Computational theories of visual perception. In Spillman, L. & Werber, J. S. (Eds), *Visual perception: The neurophysiological foundations*. London: Academic Press.

Snowden, R. J. (1992). Orientation bandwidth: The effect of spatial and temporal frequency. *Vision Research, 32*, 1965–1974.

Thomas, J. P. (1989). Independent processing of suprathreshold spatial gratings as a function of their separation in spatial frequency. *Journal of the Optical Society of America A, 6*, 1102–1111.

Tyler, C. W. & Gorea, A. (1986). Different encoding mechanisms for phase and contrast. *Vision Research, 26*, 1073–1082.

Watson, A. B. (1983). Detection and recognition of simple spatial forms. In Braddick O. J. & Sleigh A. C. (Eds), *Physical and biological processing of images*. Berlin: Springer.

Watt, R. J. (1988). *Visual processing: Computational, psychological and cognitive research*. East Sussex: Lawrence Erlbaum.

Watt, R. J. & Morgan, M. J. (1983). The recognition and representation of edge blur: Evidence for spatial primitives in human vision. *Vision Research, 23*, 1465–1477.

Watt, R. J. & Morgan, M. J. (1985). A theory of the primitive spatial code in human vision. *Vision Research, 25*, 1661–1674.

Westheimer, G. & McKee, S. P. (1977). Spatial configurations for visual hyperacuity. *Vision Research, 17*, 941–947.

Wetherill, G. B. & Levitt, H. (1965). Sequential estimation of points on a psychometric function. *British Journal of Mathematical and Statistical Psychology, 18*, 1–10.

Wilson, H. R. (1980). A transducer function for threshold and suprathreshold human vision. *Biological Cybernetics, 338*, 171–178.

Wilson, H. R. & Gelb, D. J. (1984). Modified line-element theory for spatial frequency and width discrimination. *Journal of the Optical Society of America A, 1*, 124–131.

Yuille, A. L. & Poggio, T. (1988). Scaling and fingerprint theorems for zero-crossings. In Brown C. (Ed.), *Advances in computer vision* (Vol. 2). Hillsdale, N.J.: LEA.

APPENDIX

This Appendix gives the mathematical details of the phase discrimination model and the Monte Carlo simulations presented in the discussion and Fig. 5, and is based on a model first proposed by Bennett (1993). Bennett considered a 1-D model with pairs of sine- and cosine-phase filters. However, in order to describe the results presented here, it is necessary to consider only the cosine-phase filters. Like Bennett (1993), it is assumed that the test filters respond only to the test component.

Simulations were performed on a 486PC computer, and used floating point arithmetic.

Compound detection

In compound detection, the response of an optimally placed filter (R_{cont}) is given by

$$R_{cont} = C_t + G(1) \tag{A1}$$

where C_t is the contrast of the test grating and $G(1)$ is zero-mean, unit-variance, Gaussian noise. Note that it is unnecessary to consider the effects of the contrast sensitivity function (CSF) because the model is concerned only with expressing phase-reversal discrimination relative to compound detection, and so the effects of the CSF are cancelled out.

The assumption that the visual system is able to locate the optimally placed filter for contrast (increment) detection was also made by Legge and Foley (1980).

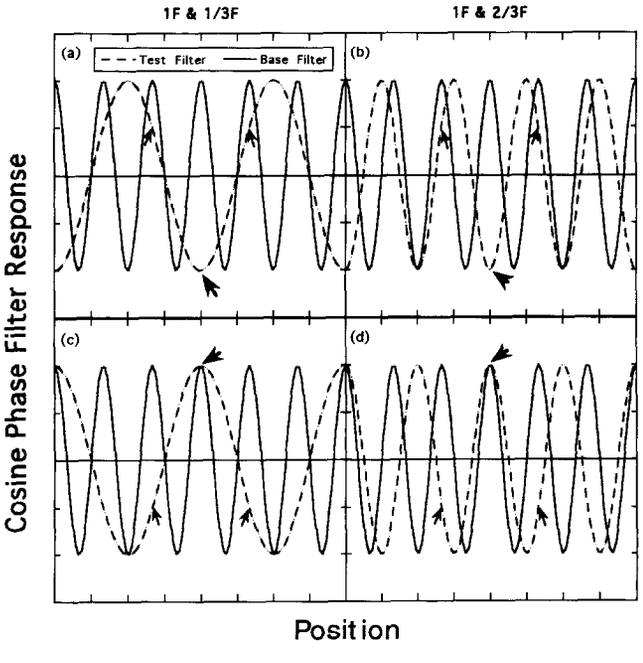

FIGURE A1. Responses of cosine-phase filters to a $1F$ base grating (solid curves) and a test grating (dashed curves) of $\frac{1}{3}F$ (A, C) and $\frac{2}{3}F$ (B, D). In (A) and (B) the base and test are in peaks-subtract phase, and in (C) and (D) the base and test are in peaks-add phase. It is assumed that the filter bandwidths are sufficiently narrow to respond only to one component of the base pattern. The arrows show the responses of the test filters centred on the peaks of the base patterns. The size of the arrows indicate the relative magnitudes of response.

Phase discrimination in 1-D

For phase discrimination in 1-D, the response of a cosine-phase test filter placed near the peak of a $1F$ base component is given by

$$R_{\text{phase1}} = C_t \cdot \cos\{2\pi f_t \cdot [G(\sigma_s) + \Phi]/f_b + \phi\} + G(1);$$
$$\Phi = \ldots -2\pi,\ 0,\ 2\pi \ldots \quad \text{(A2)}$$

where f_t and ϕ are the spatial frequency and phase of the test component, f_b is the spatial frequency of the base component, and $G(\sigma_s)$ is a Gaussian random variable that determines the accuracy with which the peak of the base component can be identified (i.e. positional jitter). $G(1)$ is zero-mean, unit-variance, Gaussian noise added to the output of the filter. The variable, Φ, determines which peak of the base pattern is used for localisation and has values only in multiples of 2π.

Decision rules at low SR ratios

When the SR ratio is an integer, then the choice of peak in the base pattern [i.e. the value of Φ in equation (A2)] is inconsequential. However, at the low noninteger SR ratios used in the experiments reported here, the choice of peak in the base pattern becomes important. For example, consider the base pattern of $1F$ illustrated in Fig. A1 with test components of $\frac{1}{3}F$ [Fig. A1 (A, C)] and $\frac{2}{3}F$ [Fig. A1 (B, D)] in peaks-subtract phase [Fig. A1 (A, B)] and peaks-add phase [Fig. A1 (C, D)]. Here, both the signs and the magnitudes of test filter responses depend on the choice of base peak (cf. large and small arrows in Fig. A1). If the unrealistic assumption is made that observers have *a priori* information about which is the optimum peak in the base pattern [i.e. those indicated by the large arrows in Fig. A1 (C, D)], then performance in phase-reversal discrimination would remain optimum for SR ratios <1. Not surprisingly this is not what was found empirically, but rather, performance deteriorated when the SF of the test pattern was decreased below that of the base pattern (see Fig. 5). Indeed, the observer does not have *a priori* knowledge of which is the optimum base peak, and so a more realistic approach is required. One possibility is to assume that the observer's behaviour is *equivalent* to applying a set of rules to the responses of three neighbouring peaks of the base pattern [Wilson and Gelb (1984) have also utilized responses from spatial neighbours]. The strategy modelled here, computed difference-responses for each of three test filters located by neighbouring base filters, and always subtracted the second interval from the first. If only one of these difference-responses was negative, then the first interval was recorded as peaks-subtract but if only one was positive, then the second interval was recorded as peaks-subtract (see Fig. A1). However, because the filter responses are noisy, there will be occasions when the three difference-responses will be either all positive or all negative. In such cases it is assumed that the observer guesses with a 50% chance of being correct.*

Finally, in order to equate the number of comparisons across all SF ratios, and also between detection and discrimination tasks, three response-differences were calculated for all tasks and conditions.

Monte Carlo simulations

Model predictions were generated by simulating 5000 pairs of 2IFC trials at each of a range of test contrasts (C_t) and at each of the SF ratios used in Expt 1. The normal deviate routine given by Press, Flannery, Teukolsky and Vetterling (1989) was used to calculate $G(\sigma_s)$ and $G(1)$ in equations (A1) and (A2), independently for each stimulus presentation. In compound detection [equation (A1)], C_t was set to zero in the second interval. In phase discrimination [equation (A2)], ϕ was set to π in the first interval and zero in the second interval. In each case, a difference response, ΔR_{cont} or ΔR_{phase}, was calculated by subtracting the second response from the first.

In compound detection, three difference responses, ΔR_{cont}, were calculated for each simulated pair of 2IFC trials using equation (A1). If the majority of difference responses was positive then the simulated behavioural response was recorded as being correct, otherwise it was incorrect. In phase discrimination, Φ was set to -2π, 0 and 2π in the three comparisons respectively. Thus, for each simulated pair of 2IFC trials, three difference responses, ΔR_{phase}, were calculated using equation (A2). When the SR ratio was >1, the simulated behavioural response was correct if the majority of these responses was negative, otherwise the response was incorrect. For SR ratios of $\frac{1}{3}$ and $\frac{2}{3}$, a correct response was recorded if one of the difference responses was negative, and an incorrect response was recorded if two of the difference responses were negative. If either none, or all three of the difference responses were negative, then the simulated behavioural response was correct with a probability of 0.5 (see previous subsection and Fig. A1).

Model thresholds were taken to be the interpolated contrast levels that produced 75% correct responses.

Phase discrimination in 2-D: independent component jitter

The model uses a peak in the base pattern to identify the spatial location of the test filter. As the test component was always a vertical grating, it is only *horizontal* localization errors that can affect model performance. In general, the horizontal jitter of a sinusoidal component of arbitrary orientation is determined by considering the spatial repetition of a horizontal slice through that component. In particular, for a sine-plaid base pattern, the horizontal spatial repetitions of the constituent components are the same as the horizontal repetition (SR_b) of the base pattern itself [i.e. they are given by $f_b \cdot \cos(\Theta)$, where Θ is the component orientation]. Consequently, if positional jitter occurs independently for each component, then for a two component sine-plaid, equation (A2) becomes

$$R_{\text{phase2i}} = C_t \cdot \cos\{2\pi f_t \cdot [(G(\sigma_s) + G(\sigma_s))/2 + \Phi]/\text{SR}_b + \phi\} + G(1);$$
$$\Phi = \ldots -2\pi,\ 0,\ 2\pi \ldots \quad \text{(A3)}$$

where the two occurrences of $G(\sigma_s)$ are evaluated independently, and SR_b is the spatial repetition of the base pattern. Note that, as in equation (A2), σ_s is the standard deviation of the jitter in the direction orthogonal to that of each of the base component orientations.

The independent component jitter shown in Fig. 5 (dashed curve) was modelled by substituting equation (A3) for equation (A2) in the Monte Carlo simulations described above.

Phase discrimination in 2-D: 100% correlated component jitter

In order to model 100% correlated component jitter for the sine-plaid condition, the second occurrence of $G(\sigma_s)$ in equation (A3) is set equal to that of the first occurrence. Thus, equation (A4) becomes

$$R_{\text{phase2c}} = C_t \cdot \cos\{2\pi f_t \cdot [G(\sigma_s) + \Phi]/\text{SR}_b + \phi\} + G(1);$$
$$\Phi = \ldots -2\pi,\ 0,\ 2\pi \ldots \quad \text{(A4)}$$

The only difference between equations (A4) and (A2) is the substitution of SR_b for f_b in equation (A4). However, in the 1-D case—when the base component is a grating—SR_b and f_b are identical, and so equations (A4) and (A2) are equivalent. Thus, a single equation (A4) can be used to model phase-reversal discrimination in both 1-D (grating condition) and 2-D (sine-plaid condition), when there is 100% correlated component jitter in the base pattern. Furthermore, so long as the model results are plotted as a function of SR ratio (rather than SF ratio), then the model predictions for the 1-D case are exactly the same as those for the 2-D case.

*An alternative strategy, and one suitable for all SR ratios, is to choose the largest of the three difference responses, and then base the behavioural response on this single difference response. An implementation of this strategy produced a model curve whose form was similar to the data, but which further underestimated phase discrimination performance at non-integer SR ratios by a few dB.